Plasma-wave generation and acceleration of electrons by a nondiverging beating optical beam

Evgeniia Ponomareva[*] and Andriy Shevchenko

Department of Applied Physics, Aalto University, P.O.Box 13500, Aalto FI-00076, Finland

Plasma waves can be used to create efficient and small-sized electron accelerators. Despite the already demonstrated success in reaching GeV-scale energy gain in the motion of electrons, laser-induced wakefields still suffer from the transverse spreading and the loss of synchronization with the accelerating particles. In this work, to tackle these problems, we propose using a two-wavelength structured laser beam with a designed angular dispersion and adjustable group velocity in free space to efficiently excite a nondiverging plasma wave. This approach allows one to generate an electron bunch with low transverse spread and reach high average acceleration gradients.

I. INTRODUCTION

Since the very beginning of laser-plasma interaction research, plasma waves have been of significant scientific and technological importance. They could open new possibilities for fusion as a heating mechanism [1,2], serve as an electron density probe [3], and even act as an efficient all-optical modulator for intense laser radiation [4]. However, the most prominent current technology based on the plasma-wave excitation (also coined as plasma wakefield excitation) is the laser-driven particle acceleration [5–14].

There are several pathways for generating plasma waves [3,5,15–18], and the laser wakefield acceleration (LWFA) is probably the most promising of them for modern applications. The LWFA mechanism is based on the excitation of a plasma wave by an intense and very short laser pulse (ideally with the duration $\tau_L < \lambda_p/c$, where λ_p is the plasma wavelength). The requirement of a high optical power is a current challenge of the LWFA schemes. An additional issue to consider is the low wall-plug efficiency of the modern ultrashort-pulse laser systems [19]. However, there are several methods that do not require fs-length pulses for plasma-wave excitation [20–22]. One of them, which serves as a basis for this work, is the plasma beat-wave acceleration (PBWA) [23,24]. The excitation in this case is resonant and provided by copropagating laser pulses with different central frequencies ω_1 and ω_2 such that

$\omega_2 - \omega_1$ approximately matches the plasma frequency ω_p. Being resonant, the method allows using lower laser powers. Since the plasma oscillation is formed by the ponderomotive force of the beating laser pulses, there is no need to make the pulse duration short. While the creation of such a pulsed two-frequency beam is a challenging task, some laser systems exhibiting this property have already been demonstrated and used for scientific purposes, especially in femtosecond pump-probe experiments [25,26]. The most notorious issue of the PBWA scheme is a loss of the resonance between the laser drive and the plasma wave. The problem, however, can be at least partially solved by choosing an optimal frequency mismatch [27] or using certain pulse-chirping schemes [28,29].

In practice, all plasma-wave excitation and acceleration mechanisms using high-intensity (focused) light pulses share the same diffraction and dephasing problems. Focused laser beams inevitably spread, which limits the light-plasma interaction length to a few Rayleigh ranges. The diffraction problem can be solved with the help of relativistic self-focusing [30] or an optical waveguide [31,32]. For instance, a meter-scale laser-generated plasma channel has been demonstrated to guide high-intensity laser light [31]. Recently, using these all-optical plasma waveguide structures, efficient electron acceleration, up to a GeV level energy, has been achieved [32].

The other issue, the dephasing, is caused by a mismatch between the electron and wakefield velocities. For the acceleration to be efficient, the electrons must "ride" the wake as a surfer rides the water wave. However, the real outcome is that they outrun the wake after propagating over the so-called dephasing length $L_d^{3D} = 4\omega_0^2\sqrt{a_0}/3\omega_p^2 k_p$ [9], where ω_0 is the central angular frequency of the laser beam and k_p is the plasma wave number. To make the intensity peaks accelerate together with the electrons, the

*evgeniia.a.ponomareva@aalto.fi

conventional LWFA scheme was combined with a spatio-temporal shaping of the laser pulse [33]. A similar approach was reported in [34], where quasi-Bessel beams with designed spatiotemporal profiles were successfully utilized to unlock the dephasing-free regime with a more than tenfold increase in the electron beam energy gain.

The goal of this paper is to show that a pulsed Bessel-Gauss beam that exhibits the wave beating phenomenon is capable to drive essentially nondiverging high-amplitude plasma waves with adjustable speed. This can not only eliminate the need for the creation and control of plasma waveguide structures but also allow monitoring of the possible velocity mismatch between the electrons and the wakefield without any specific optical equipment.

II. THE APPROACH

As illustrated in Fig. 1(a), our wakefield generation approach relies on a two-color optical field, with angular frequencies ω_1 and ω_2 significantly exceeding ω_p, focused into an underdense plasma by an axicon. The ponderomotive force of the beating light resonantly drives plasma waves that propagate with a phase velocity approximately equal to the group velocity of the driving light. To the first order, the speed of the plasma wave is $v \approx c(1 - \omega_p^2/2\omega_1\omega_2)$, where c is the speed of light in vacuum. Thus, in the case of a plane-wave excitation, the
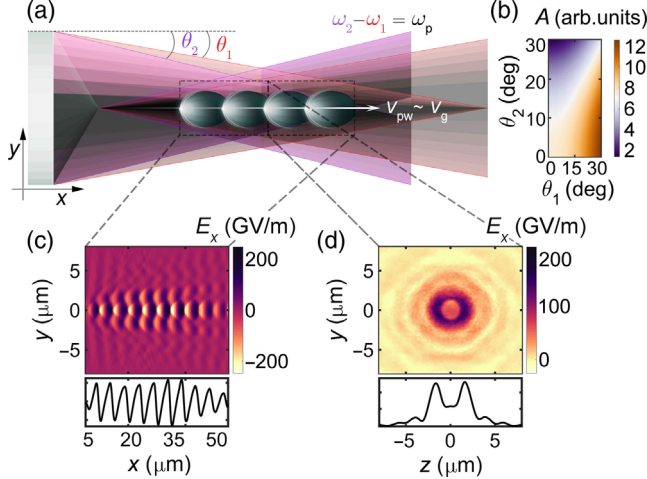

FIG. 1. Plasma wave excited by a beating Bessel-Gauss beam. (a) Schematic of the approach. Here, a two-color optical beam is converted by an axicon to a nondiverging beam to excite the plasma wakefield; θ_1 and θ_2 are the deflection angles of the components with frequencies ω_1 and ω_2, respectively, at the axicon. (b) The angular distribution of the plasma wave amplitude (A) obtained from an approximate 1D analysis. The results of the 3D particle-in-cell simulations: (c) the longitudinal electric-field distribution of the excited plasma wave in the xy-plane crossing the beam center and (d) the distribution of the field in the yz-plane in the middle of the Bessel-Gauss beam. The curves at the bottom of (c) and (d) are the field profiles at $y = 0$.

velocity of the wave is always slightly below the speed of light in vacuum. However, the group velocity and even acceleration of a two-color Bessel beam can be adjusted [35,36], which provides the possibility to control the speed mismatch between the axial optical and plasma waves. The group velocity in such a Bessel beam is determined by the propagation angles θ_1 and θ_2 of the plane-wave components of the beam at the two frequencies, ω_1 and ω_2, respectively (see Fig. 1). It is given by [35,36].

$$v_g/c_p = \frac{\omega_2 - \omega_1}{\omega_2 \cos\theta_2 - \omega_1 \cos\theta_1}, \quad (1)$$

where $c_p = c/n_p = c/\sqrt{1 - \omega_p^2/\omega_1\omega_2}$ is the phase velocity of light in the plasma. The group velocity can be higher than c_p (superluminal), lower than c_p (subluminal), or even negative, also in free space [35,36].

For an ordinary transmissive axicon, the angles θ_1 and θ_2 are determined by the dispersion of the axicon material that, for the application proposed here, must have a high optical damage threshold. It is also possible to design a diffractive axicon or a meta-axicon that provides prescribed angles θ_1 and θ_2 for prescribed wavelengths λ_1 and λ_2 (see, e.g., [37,38]). When dealing with high optical powers ($> 10^{14}$ W/cm^2), reflective axicons (either smooth conical or flat diffractive mirrors) would be preferable. For a reflective diffractive axicon, we normally have $\theta_1 > \theta_2$ for $\lambda_1 > \lambda_2$, which is required to obtain a luminal or a superluminal group velocity. In addition, two Bessel beams with different wavelengths can be created separately and combined into a single double-wavelength beam. We also point out that a Bessel beam can be created without an axicon by Fourier transforming a ring-shaped intensity profile using a lens.

Using a 1D analysis presented in [15] for the wake excitation by a beating optical wave in a cold homogeneous plasma, one can obtain the amplitude growth rate of the plasma wave as $\gamma = a_1 a_2 \Delta k c^2/4\omega_p$, with $a_{1,2} = eE_{1,2}/m_e c\omega_{1,2}$ being a peak amplitude of the normalized dimensionless vector potential in a gauge with the scalar potential equal to zero [18], and $\Delta k = \frac{1}{c}(\omega_2 \cos\theta_2 - \omega_1 \cos\theta_1)$. Obviously, the amplitude increases proportionally to Δk. The calculated dependence of the plasma-wave amplitude on angles θ_1 and θ_2 is presented in Fig. 1(b) (see the Appendix for the 1D analysis details).

The 1D analysis suggests that the plasma wave amplitude can be increased by adjusting the angles of the beam plane-wave components. Therefore, to obtain a more realistic picture, we performed particle-in-cell simulations using a 3D massively parallel code EPOCH [39]. The excitation beam is assumed to be linearly polarized and propagating in the positive x direction. As a target, we used a fully ionized cold electron plasma with a uniform density

of $n_0 = 4.5 \times 10^{19}$ cm^{-3}. To satisfy the resonance condition for the wakefield excitation at this density, we selected the wavelengths of the beam components as $\lambda_1 = 1$ μm and $\lambda_2 = 0.833$ μm. In the simulations, we used a realistic Bessel-Gauss beam instead of an infinitely wide Bessel beam. The Gaussian envelope was taken in the form $\exp(-r^2/w^2)$, where $w = 15$ μm. The Bessel-Gauss beam is obtained by adding the radially varying phase $\phi(r) = 2\pi r \sin\theta_i/\lambda_i$ to each component i of the Gaussian beam [40]. The considered interaction length of the beam with the plasma (along x) was taken to be 50 μm. The beam was assumed to be pulsed, with the pulse duration of 100 fs and the intensities of 5×10^{15} W/cm^2 for each frequency component. The pulse duration is chosen rather arbitrarily, to make the simulation time reasonably short and simultaneously have the parameter values achievable in an experiment. All other parameters and simulation details are listed in Table I.

To start with, we consider the case of $\theta_1 = \theta_2 = 15°$. In Fig. 1, subfigures (c) and (d) present the longitudinal and transverse profiles of the electric-field component E_x of the plasma wave at a fixed instant of time. The plasma wave follows the profile of the Bessel-Gauss beam and does not diverge. If a Gaussian beam of the same waist radius was used, its diameter would increase to ca. 15 μm upon propagation over a distance of 50 μm, and the peak power would drop by more than 50 times. Hence, if a focused laser beam is to be used, a Bessel-Gauss beam could be a better option, allowing the laser spot size to be small and the intensity to be high within a large propagation distance. This, however, requires the total power of the beam to be increased. In the case considered here, the maximum total power of the Bessel-Gauss beam is larger than that of the corresponding Gaussian beam by a factor of 2. This factor would be equal to about 10 if the Gaussian envelope of the Bessel-Gauss beam had a radius of 1 mm.

TABLE I.   Simulation parameters.

Parameter	Value
Box size, $x \times y \times z$	$65 \times 25 \times 25$ μm^3
Number of grid points	
$n_x \times n_y \times n_z$	$1200 \times 450 \times 450$
Time step Δt, defined	
by the CFL condition:	$0.95 = c\Delta t/\Delta x$, $\Delta x = x/n_x$
Particles per cell	4
Plasma length	50 μm
Plasma density	4.5×10^{19} cm^{-3}
Pump wavelengths, λ_1, λ_2	1 μm, 0.833 μm
Pump intensity, $I_{1,2}$	5×10^{15} W cm^{-2}
Pulse temporal profile	$\exp[-(t-t_0)^2/T^2]$, $T = 100$ fs
Pulse spatial profile	$\exp(-r^2/w^2)$, $w = 15$ μm
Profile of component i [40]	$\phi(r) = 2\pi r \sin\theta_i/\lambda_i$, $i = 1, 2$

III. TRADE-OFF BETWEEN THE BEAT-WAVE AND PLASMA-WAVE VELOCITIES

To obtain information about the dependence of the plasma-wave excitation efficiency on both angles θ_1 and θ_2 of the beam components, we calculate E_x for several sets of the angles [see the crosses in Fig. 2(a)]. The data were then interpolated, resulting in a smooth distribution of E_x in the upper plot of Fig. 2(a). The distribution is not symmetric, suggesting that the optimal values of θ_1 and θ_2 can be different, i.e., $\theta_1 \neq \theta_2$. The lower plot in Fig. 3(a) shows the distribution of the group velocity in the same angular range, calculated using Eq. (1). We recall that the on-axis group velocity of a beam can be higher than the speed of light in vacuum [35,36]. It can be seen that E_x is maximized when the on-axis group velocity of the beam is close to the plasma-wave velocity, which is $v \approx 0.98$ c for the electron density used here. This happens when $\theta_1 \approx 1.1\theta_2$. If this condition is not fulfilled, a dephasing of the laser and plasma waves occurs, and a further increase in E_x becomes impossible.

Let us next increase the light intensity and analyze the electron density perturbation along with the kinetic energy of the electrons, $\mathcal{E}$. We calculate the energy density distributions of the accelerated electrons, $\mathcal{E}n$, for a subluminal group velocity of the driver beam [$v_g/c \approx 0.91$, Figs. 2(b)–2(d)] and for the case of $v_g/c \approx 1$ [see Figs. 3(e)–(g)]. The peak intensity of each frequency component $I_0^{1,2}$ is increased from 10^{16} W/cm^2 to 10^{17} W/cm^2 in both simulation sets. The wave-breaking limit of the electric field of the plasma wave [18], $E_{wb} \approx 96\sqrt{n_0(cm^{-3})} \approx 600$ GV/m, was reached already at 5×10^{16} W/cm^2 (the corresponding peak vector potentials in the Bessel-Gauss beam are $a_1 = a_2 > 1$ at this intensity value). At this point, the self-injected electrons are "blown out" from the cavitation area.

The electron density perturbation is larger for the subluminal regime [Figs. 2(b)–(d)]. As a result, the electrons are accelerated with a pronounced transverse spread. As described in [41], this propagation regime results in unwanted injection and trapping of the particles, reducing the acceleration field and increasing the divergence of the electron bunch. For $v_g/c \approx 1$, the energy gain is considerably higher and the electron spread is low [see Fig. 2(e)–(g); note that the energy density distributions are plotted in a logarithmic scale]. Thereby, the PBWA scheme based on the designed angular dispersion helps to control the characteristics of the accelerated electrons.

To look into more details on the mismatch between the laser field and the plasma wave, we have studied the time-resolved evolution of the plasma density peak for the cases of luminal, subluminal, and superluminal propagation regimes of the light field. Figures 3(a)–3(c) illustrate the temporal evolution of the density perturbation overlapped with the beat-wave longitudinal electric field profile, while
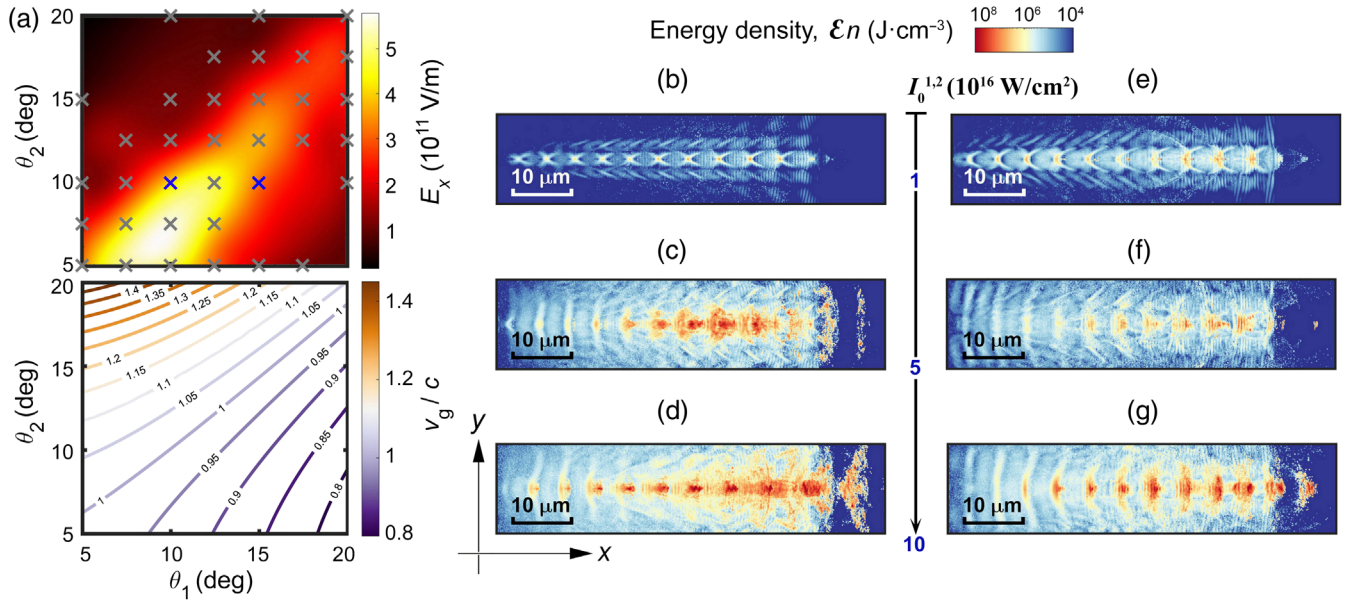
FIG. 2. Plasma wakefield excitation via the controlled group velocity. (a) The upper plot shows the plasma wake amplitude E_x as a function of θ_1 and θ_2 obtained by interpolating the simulation data. The cross symbols correspond to the values extracted directly from the simulation. The lower plot shows the distribution of the group velocity calculated using Eq. (1). (b–d) The energy density profiles in a logarithmic scale for $\theta_1 = 15°$ and $\theta_2 = 10°$, corresponding to $v_g/c \approx 0.91$. (e–g) The same as in (b–d), but for $\theta_1 = \theta_2 = 10°$, corresponding to $v_g/c \approx 1$. The cases (b–d) and (e–g) are additionally highlighted in (a) by the blue-colored cross symbols. The intensity of both frequency components takes the values of 10^{16} W/cm² in (b) and (e), 5×10^{16} W/cm² in (c) and (f), and 10^{17} W/cm² in (d) and (g). The data are shown at the instant of time 0.1 ps after the pulse center matched the center of the plasma.
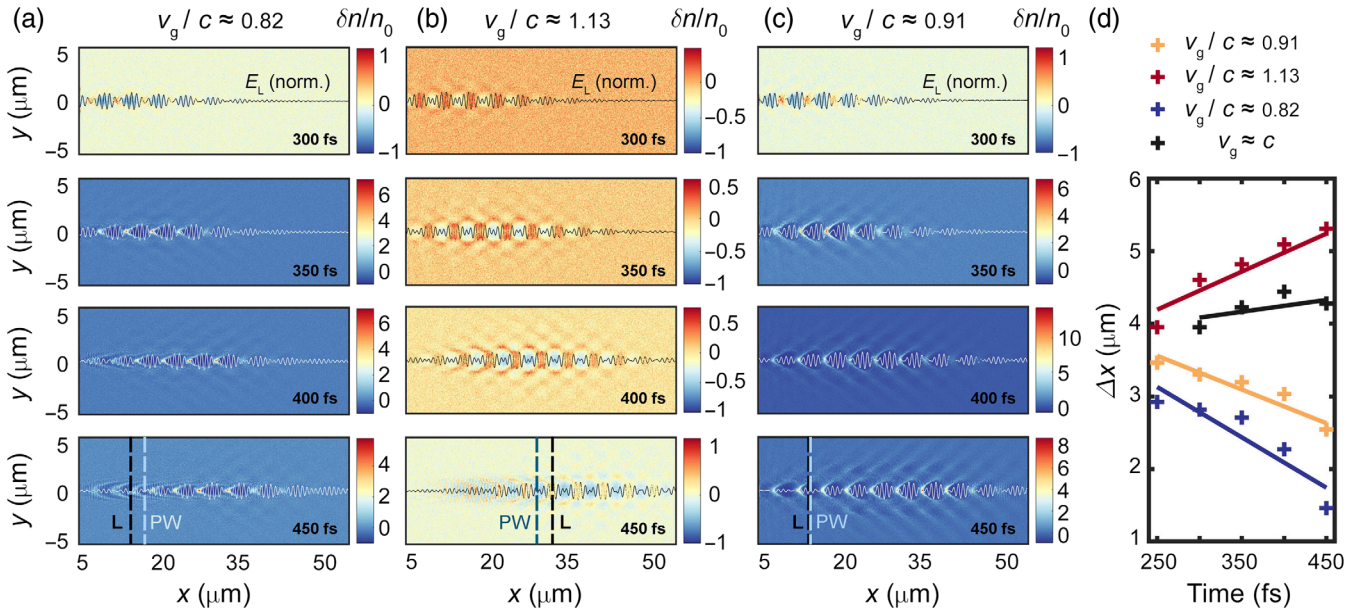

FIG. 3. Plasma wakefield driven by a Bessel-Gauss laser beat-wave with adjustable group velocity. In each plot, the electron density perturbation $\delta n/n_0$ and the longitudinal electric field E_L of the laser are shown. (a) $v_g/c \approx 0.82$—plasma wave outruns the beat wave, (b) $v_g/c \approx 1.13$—plasma wave lags behind the beat wave, (c) $v_g/c \approx 0.91$—plasma wave slightly outruns the beat wave. The cyan/blue and black dashed lines are the indicators of the delay between the plasma wave and the laser intensity peaks. (d) Time-resolved evolution of the density peak with respect to the beat-wave maximum for the cases (a–c) compared to the luminal propagation.

Fig. 3(d) summarizes the observed dynamics and provides a comparison of the different propagation regimes. It can be seen that the phase velocity slippage of the plasma wave for the superluminal case is so strong that no efficient wave excitation is observed at any instance of time. As Fig. 3(d) illustrates, the slope is the smallest for the case of $v_g \approx c$.

IV. ELECTRON ACCELERATION

Figure 4(a) compares the energy spectra obtained by analyzing the accelerating electrons at the output of the plasma in Figs. 2(d) and 2(g). The beam with $v_g \approx c$ is clearly more efficient than the beam with $v_g/c \approx 0.91$. However, the angular spread of the accelerated electrons is approximately the same in the two cases [see Fig. 4(b)]. The width of the profile corresponds to the average deviation of 11.5° of the direction of the electron motion from the y axis. This corresponds to the values of angles θ_1 and θ_2, suggesting that the angular spread of the accelerated electrons approximately matches the angular spread of the accelerating beams. In other words, the electrons are accelerated by the plane-wave components of the Bessel-Gauss beams. However, we still observe a significantly reduced transverse spread of the accelerated electrons for $v_g \approx c$, which implies that the acceleration is more efficient near the beam axis at this particular group velocity.

Staying in the high-intensity regime, $I_0^{1,2} = 5 \times 10^{16}$ W/cm², we next address the wakefield-based acceleration process by changing θ_1 and keeping θ_2 at 7.5°. By doing so, we tune the group velocity of the two-color Bessel-Gauss beam from subluminal to superluminal in the region of maximized E_x [see Fig. 2(a)]. Figures 5(a)–5(c) shows the velocity-dependent curves for the kinetic energy $\mathcal{E}$, standard deviation σ of the transverse coordinate from the beam center, and the relative density perturbation $\delta n/n_0$. We observe a direct correlation between the electron density perturbation [Fig. 5(c)] and the bunch divergence [Fig. 5(b)]. Moreover, the decrease in the energy gain at

$v_g/c < 1$ is partly at odds with the enhancement of the plasma-wave electric field shown in Fig. 2(a). We see that, while it is preferable to have a subluminal group velocity of the driver beam to maximize the plasma-wave amplitude, the reduction of the electron bunch size favors a super-luminal regime. Hence, a group velocity equal to the speed of light in vacuum can be considered a trade-off for generating highly energetic electrons with reduced trans-verse spread via a two-color Bessel-Gauss beam. We compare these parameters with those obtained when using a Gaussian PBWA (see the dashed line in Fig. 5). The waist and the peak electric field of the Gaussian beam were adjusted to match the characteristics of the Bessel-Gauss beam. In the considered case, the pulse underwent self-focusing and experienced subsequent transverse spreading, losing the energy. We think that a proper increase in the peak intensity can lead to a more efficient self-channeling of the pulse. However, the self-channeling caused by the self-phase modulation of the beam will be sensitive to fluctuations of the beam power, while a Bessel-Gauss beam-driven wakefield will be naturally divergence-free and more stable. Another key point is that Gaussian-beam-driven PBWA will face a dephasing limit in a short propagation distance, while a structured beam makes it possible to avoid this problem. We also emphasize that laser beams used in such electron accelerators typically have a diameter of several tens of micrometers or larger, and the transverse spread of the accelerated electrons is

FIG. 5. Dependence of PBWA parameters on θ_1 at fixed $\theta_2 = 7.5°$: (a) electron energy $\mathcal{E}$, (b) standard deviation of electron position σ, and (c) density perturbation $\delta n/n_0$. The dashed line indicates the values obtained for the Gaussian PBWA with the same beam diameter and peak intensity. The green rectangle highlights a range of optimal values of θ_1.
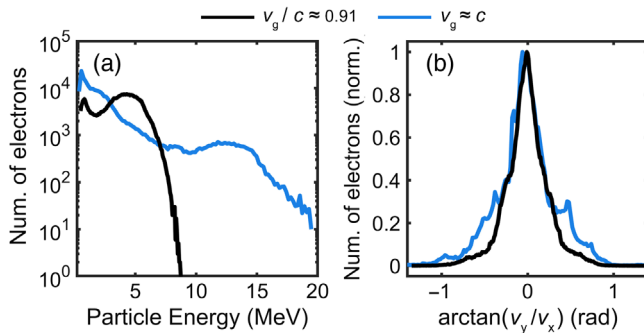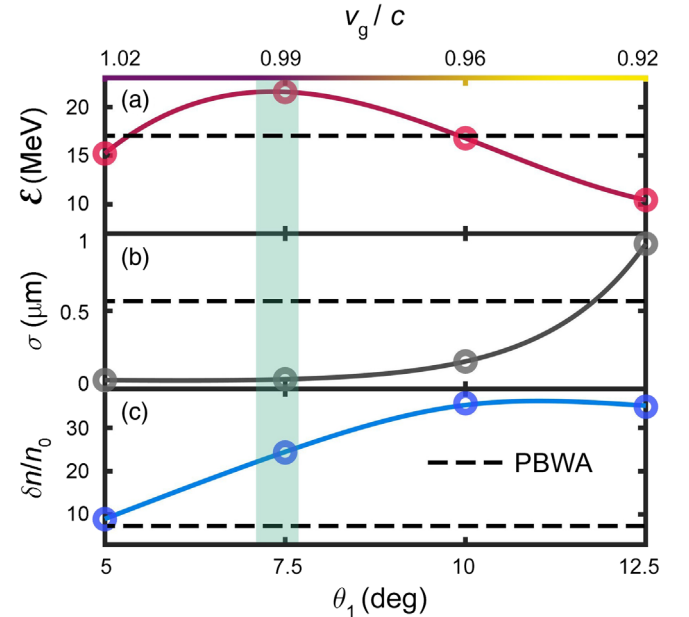

FIG. 4. The histograms for the electron (a) energy and (b) angular spread. The results presented in these plots correspond to the same simulation setup that was used for obtaining the data in Figs. 2(d) and 2(g). In (b), the number of electrons is normalized to its maximum value.

therefore the same as the beam diameter or larger. Such diameters are used to make the Rayleigh range of the beam comparable to or larger than the acceleration length. When a Bessel-Gauss beam is used, the beam diameter can be much smaller and the Rayleigh range is essentially unlimited. For example, the Bessel beam used in our calculations (with a radius of 2 μm only) can easily be made to remain propagation-invariant over a distance of 10 mm, making it possible to achieve much smaller electron spreads.

V. CONCLUSIONS

We have proposed an approach to generate a plasma wakefield by the resonant interaction of plasma with a beating dual-color structured optical beam. The approach is capable of exciting nondiverging Bessel-like plasma waves and producing electron bunches with low transverse spread. The method can be used with other structured beams as well and at any electron density. However, it should be taken into account that the dephasing length is smaller at higher electron densities. One should therefore carefully select n_e to allow for a long acceleration distance able to produce monoenergetic electrons [6]. Moreover, the group velocity of laser light in a dual-frequency Bessel beam can be made dependent on the distance of propagation [35,36], which can be used to compensate for the dephasing. We expect this scheme to be experimentally examined in the near future for efficient operation over a few-mm acceleration distance.

ACKNOWLEDGMENTS

APPENDIX: ONE-DIMENSIONAL MODEL OF PLASMA WAVE EXCITATION BY BEATING BESSEL BEAM PULSES

We analyze the excitation and amplitude enhancement of a plasma wave by a beating Bessel beam of pulsed light, using an analytical theory proposed by Rosenbluth and Liu in [15]. This theory considers a one-dimensional problem of the interaction of plasma with light. The monochromatic plane-wave components of the considered Bessel beams are $E_1 \sin(k_1 z \cos\theta_1 - \omega_1 t)$ and $E_2 \sin(k_2 z \cos\theta_2 - \omega_2 t)$, where $\omega_2 - \omega_1 = \omega_p$. The goal is to find a response of the cold homogeneous plasma to the total electric field of the two waves. For this, we solve the following equation for the electron displacement δ_x [15]:

$$\frac{\partial^2 \delta_x}{\partial t^2} + \omega_p^2 \delta_x = \frac{e}{m_e c}(v_{y1} B_{z2} + v_{y2} B_{z1}), \quad \text{(A1)}$$

where B_{zi} is the z component of the magnetic flux density of component i of the beam and $v_{yi} = -\frac{e}{2m_e \omega_i} E_i \exp[i(k_i z \cos\theta_i - \omega_i t) + \text{c.c.}]$ is the y component of the velocity vector obtained by solving the fluid momentum equation. Considering the ansatz in the form $\delta_x(x_0, t) = A(t)\sin[k_0 x_0 - \omega_p t + \phi(t)]$, we obtain the equations

$$\frac{\partial A}{\partial t} = -\alpha \sin[\phi + x_0(k_0 - \Delta k)], \quad \text{(A2)}$$

$$A\frac{\partial \phi}{\partial t} = -\alpha \cos[\phi + x_0(k_0 - \Delta k)], \quad \text{(A3)}$$

which are similar to those derived in [15]. Here, we have $\alpha = a_1 a_2 \Delta k c^2 / 4\omega_p$, with a_1 and a_2 being the normalized vector potentials (see the main text), and $\Delta k = k_2 \cos\theta_2 - k_1 \cos\theta_1$. The stationary phase solution provides the growth rate of the plasma-wave amplitude of $\gamma = a_1 a_2 \Delta k c^2 / 4\omega_p$. This solution is plotted in Fig. 1(b) of the article.

[1] B. I. Cohen, A. N. Kaufman, and K. M. Watson, Beat Heating of a Plasma, Phys. Rev. Lett. **29,** 581 (1972).

[2] D. W. Forslund, J. M. Kindel, W. B. Mori, C. Joshi, and J. M. Dawson, Two-Dimensional Simulations of Single-Frequency and Beat-Wave Laser-Plasma Heating, Phys. Rev. Lett. **54,** 558 (1985).

[3] N. M. Kroll, A. Ron, and N. Rostoker, Optical Mixing as a Plasma Density Probe, Phys. Rev. Lett. **13,** 83 (1964).

[4] L.-L. Yu, Y. Zhao, L.-J. Qian, M. Chen, S.-M. Weng, Z.-M. Sheng, D. Jaroszynski, W. Mori, and J. Zhang, Plasma optical modulators for intense lasers, Nat. Commun. **7,** 11893 (2016).

[5] T. Tajima and J. M. Dawson, Laser Electron Accelerator, Phys. Rev. Lett. **43,** 267 (1979).

[6] S. P. Mangles, C. Murphy, Z. Najmudin, A. G. R. Thomas, J. Collier, A. E. Dangor, E. Divall, P. Foster, J. Gallacher, C. Hooker *et al.*, Monoenergetic beams of relativistic electrons from intense laser–plasma interactions, Nature (London) **431,** 535 (2004).

[7] C. Geddes, C. Toth, J. Van Tilborg, E. Esarey, C. Schroeder, D. Bruhwiler, C. Nieter, J. Cary, and W. Leemans, High-quality electron beams from a laser wakefield accelerator using plasma-channel guiding, Nature (London) **431,** 538 (2004).

[8] J. Faure, Y. Glinec, A. Pukhov, S. Kiselev, S. Gordienko, E. Lefebvre, J.-P. Rousseau, F. Burgy, and V. Malka, A laser–plasma accelerator producing monoenergetic electron beams, Nature (London) **431,** 541 (2004).

[9] W. Lu, M. Tzoufras, C. Joshi, F. S. Tsung, W. B. Mori, J. Vieira, R. A. Fonseca, and L. O. Silva, Generating multi-GeV electron bunches using single stage laser wakefield acceleration in a 3D nonlinear regime, Phys. Rev. ST Accel. Beams **10,** 061301 (2007).

[10] C. E. Clayton, J. E. Ralph, F. Albert, R. A. Fonseca, S. H. Glenzer, C. Joshi, W. Lu, K. A. Marsh, S. F. Martins, W. B. Mori, A. Pak, F. S. Tsung, B. B. Pollock, J. S. Ross, L. O. Silva, and D. H. Froula, Self-Guided Laser Wakefield Acceleration beyond 1 GeV Using Ionization-Induced Injection, Phys. Rev. Lett. **105,** 105003 (2010).

[11] J. L. Shaw, N. Lemos, L. D. Amorim, N. Vafaei-Najafabadi, K. A. Marsh, F. S. Tsung, W. B. Mori, and C. Joshi, Role of Direct Laser Acceleration of Electrons in a Laser Wakefield Accelerator with Ionization Injection, Phys. Rev. Lett. **118,** 064801 (2017).

[12] A. Döpp, C. Thaury, E. Guillaume, F. Massimo, A. Lifschitz, I. Andriyash, J.-P. Goddet, A. Tazfi, K. Ta Phuoc, and V. Malka, Energy-Chirp Compensation in a Laser Wakefield Accelerator, Phys. Rev. Lett. **121,** 074802 (2018).

[13] E. Gschwendtner and P. Muggli, Plasma wakefield accelerators, Nat. Rev. Phys. **1,** 246 (2019).

[14] L. T. Ke, K. Feng, W. T. Wang, Z. Y. Qin, C. H. Yu, Y. Wu, Y. Chen, R. Qi, Z. J. Zhang, Y. Xu, X. J. Yang, Y. X. Leng, J. S. Liu, R. X. Li, and Z. Z. Xu, Near-GeV Electron Beams at a few Per-Mille Level from a Laser Wakefield Accelerator via Density-Tailored Plasma, Phys. Rev. Lett. **126,** 214801 (2021).

[15] M. Rosenbluth and C. Liu, Excitation of Plasma Waves by Two Laser Beams, Phys. Rev. Lett. **29,** 701 (1972).

[16] R. J. Noble, Plasma-wave generation in the beat-wave accelerator, Phys. Rev. A **32,** 460 (1985).

[17] J. Krall, A. Ting, E. Esarey, and P. Sprangle, Enhanced acceleration in a self-modulated-laser wake-field accelerator, Phys. Rev. E **48,** 2157 (1993).

[18] E. Esarey, C. B. Schroeder, and W. P. Leemans, Physics of laser-driven plasma-based electron accelerators, Rev. Mod. Phys. **81,** 1229 (2009).

[19] F. Albert, M. Couprie, A. Debus, M. C. Downer, J. Faure, A. Flacco, L. A. Gizzi, T. Grismayer, A. Huebl, C. Joshi *et al.*, 2020 roadmap on plasma accelerators, New J. Phys. **23,** 031101 (2021).

[20] P. King, K. Miller, N. Lemos, J. Shaw, B. Kraus, M. Thibodeau, B. Hegelich, J. Hinojosa, P. Michel, C. Joshi *et al.*, Predominant contribution of direct laser acceleration to high-energy electron spectra in a low-density self-modulated laser wakefield accelerator, Phys. Rev. Accel. Beams **24,** 011302 (2021).

[21] P. Tomassini, D. Terzani, L. Labate, G. Toci, A. Chance, P. A. P. Nghiem, and L. A. Gizzi, High quality electron bunches for a multistage GeV accelerator with resonant multipulse ionization injection, Phys. Rev. Accel. Beams **22,** 111302 (2019).

[22] O. Jakobsson, S. M. Hooker, and R. Walczak, GeV-Scale Accelerators Driven by Plasma-Modulated Pulses from Kilohertz Lasers, Phys. Rev. Lett. **127,** 184801 (2021).

[23] V. Stefan, B. Cohen, and C. Joshi, Nonlinear mixing of electromagnetic waves in plasmas, Science **243,** 494 (1989).

[24] Y. Kitagawa, T. Matsumoto, T. Minamihata, K. Sawai, K. Matsuo, K. Mima, K. Nishihara, H. Azechi, K. A. Tanaka, H. Takabe, and S. Nakai, Beat-Wave Excitation of Plasma Wave and Observation of Accelerated Electrons, Phys. Rev. Lett. **68,** 48 (1992).

[25] A. Gambetta, G. Galzerano, A. Rozhin, A. Ferrari, R. Ramponi, P. Laporta, and M. Marangoni, Sub-100 fs

[26] two-color pump-probe spectroscopy of single wall carbon nanotubes with a 100 MHz Er-fiber laser system, Opt. Express **16,** 11727 (2008).

[26] T. Hansel, G. Steinmeyer, R. Grunwald, C. Falldorf, J. Bonitz, C. Kaufmann, V. Kebbel, and U. Griebner, Synthesized femtosecond laser pulse source for two-wavelength contouring with simultaneously recorded digital holograms, Opt. Express **17,** 2686 (2009).

[27] C. Tang, P. Sprangle, and R. Sudan, Dynamics of space-charge waves in the laser beat wave accelerator, Phys. Fluids **28,** 1974 (1985).

[28] M. Deutsch, B. Meerson, and J. E. Golub, Strong plasma wave excitation by a "chirped" laser beat wave, Phys. Fluids B **3,** 1773 (1991).

[29] R. R. Lindberg, A. E. Charman, J. S. Wurtele, and L. Friedland, Robust Autoresonant Excitation in the Plasma Beat-Wave Accelerator, Phys. Rev. Lett. **93,** 055001 (2004).

[30] P. Sprangle, E. Esarey, A. Ting, and G. Joyce, Laser wakefield acceleration and relativistic optical guiding, Appl. Phys. Lett. **53,** 2146 (1988).

[31] B. Miao, L. Feder, J. E. Shrock, A. Goffin, and H. M. Milchberg, Optical Guiding in Meter-Scale Plasma Waveguides, Phys. Rev. Lett. **125,** 074801 (2020).

[32] K. Oubrerie, A. Leblanc, O. Kononenko, R. Lahaye, I. A. Andriyash, J. Gautier, J.-P. Goddet, L. Martelli, A. Tafzi, K. Ta Phuoc *et al.*, Controlled acceleration of GeV electron beams in an all-optical plasma waveguide, Light Sci. Appl. **11,** 180 (2022).

[33] J. P. Palastro, J. L. Shaw, P. Franke, D. Ramsey, T. T. Simpson, and D. H. Froula, Dephasingless Laser Wakefield Acceleration, Phys. Rev. Lett. **124,** 134802 (2020).

[34] C. Caizergues, S. Smartsev, V. Malka, and C. Thaury, Phase-locked laser-wakefield electron acceleration, Nat. Photonics **14,** 475 (2020).

[35] P. Hildén, E. Ilina, M. Kaivola, and A. Shevchenko, Multifrequency bessel beams with adjustable group velocity and longitudinal acceleration in free space, New J. Phys. **24,** 033042 (2022).

[36] E. Ilina, P. Hildén, M. Kaivola, and A. Shevchenko, Continuous wave bessel beams with a strong longitudinal acceleration in free space, Opt. Lett. **47,** 4060 (2022).

[37] F. Aieta, P. Genevet, M. A. Kats, N. Yu, R. Blanchard, Z. Gaburro, and F. Capasso, Aberration-free ultrathin flat lenses and axicons at telecom wavelengths based on plasmonic metasurfaces, Nano Lett. **12,** 4932 (2012).

[38] W. T. Chen, M. Khorasaninejad, A. Y. Zhu, J. Oh, R. C. Devlin, A. Zaidi, and F. Capasso, Generation of wavelength-independent subwavelength Bessel beams using metasurfaces, Light **6,** e16259 (2017).

[39] T. Arber, K. Bennett, C. Brady, A. Lawrence-Douglas, M. Ramsay, N. Sircombe, P. Gillies, R. Evans, H. Schmitz, A. Bell *et al.*, Contemporary particle-in-cell approach to laser-plasma modelling, Plasma Phys. Controlled Fusion **57,** 113001 (2015).

[40] K. Ardaneh, R. Giust, B. Morel, and F. Courvoisier, Generation of a bessel beam in FDTD using a cylindrical antenna, Opt. Express **28,** 2895 (2020).

[41] J. Palastro, B. Malaca, J. Vieira, D. Ramsey, T. Simpson, P. Franke, J. Shaw, and D. Froula, Laser-plasma acceleration beyond wave breaking, Phys. Plasmas **28,** 013109 (2021).